germline mutation and a somatic mutation in PIGT. Blood 122(7): 1312–1315. doi:10.1182/blood-2013-01-481499
12. Kvarnung M, Nilsson D, Lindstrand A, Korenke GC, Chiang SC, Blennow E, Bergmann M, Stodberg T, Makitie O, Anderlid BM, Bryceson YT, Nordenskjold M, Nordgren A (2013) A novel intellectual disability syndrome caused by GPI anchor deficiency due to homozygous mutations in PIGT. J Med Genet 50(8):521–528. doi: 10.1136/jmedgenet-2013-101654
13. DePristo MA, Banks E, Poplin R, Garimella KV, Maguire JR, Hartl C, Philippakis AA, del Angel G, Rivas MA, Hanna M, McKenna A, Fennell TJ, Kernytsky AM, Sivachenko AY, Cibulskis K, Gabriel SB, Altshuler D, Daly MJ (2011) A framework for variation discovery and genotyping using next-generation DNA sequencing data. Nat Genet 43(5):491–498. doi:10.1038/ng.806
14. Wang K, Li M, Hakonarson H (2010) ANNOVAR: functional annotation of genetic variants from high-throughput sequencing data. Nucleic Acids Res 38(16):e164. doi:10.1093/nar/gkq603
15. Adzhubei IA, Schmidt S, Peshkin L, Ramensky VE, Gerasimova A, Bork P, Kondrashov AS, Sunyaev SR (2010) A method and server for predicting damaging missense mutations. Nat Methods 7(4):248–249. doi:10.1038/nmeth0410-248
16. Schwarz JM, Rodelsperger C, Schuelke M, Seelow D (2010) MutationTaster evaluates disease-causing potential of sequence alterations. Nat Methods 7(8):575–576. doi:10.1038/nmeth0810-575
17. Ohishi K, Inoue N, Kinoshita T (2001) PIG-S and PIG-T, essential for GPI anchor attachment to proteins, form a complex with GAA1 and GPI8. EMBO J 20(15):4088–4098. doi:10.1093/emboj/20.15.4088
18. Ashida H, Hong Y, Murakami Y, Shishioh N, Sugimoto N, Kim YU, Maeda Y, Kinoshita T (2005) Mammalian PIG-X and yeast Pbn1p are the essential components of glycosylphosphatidylinositol-mannosyltransferase I. Mol Biol Cell 16(3):1439–1448. doi:10.1091/mbc.E04-09-0802
19. Genomes Project C, Abecasis GR, Altshuler D, Auton A, Brooks LD, Durbin RM, Gibbs RA, Hurles ME, McVean GA (2010) A map of human genome variation from population-scale sequencing. Nature 467(7319):1061–1073. doi:10.1038/nature09534
20. Genomes Project C, Abecasis GR, Auton A, Brooks LD, DePristo MA, Durbin RM, Handsaker RE, Kang HM, Marth GT, McVean GA (2012) An integrated map of genetic variation from 1,092 human genomes. Nature 491(7422):56–65. doi:10.1038/nature11632
21. Murakami Y, Kanzawa N, Saito K, Krawitz PM, Mundlos S, Robinson PN, Karadimitris A, Maeda Y, Kinoshita T (2012) Mechanism for release of alkaline phosphatase caused by glycosylphosphatidylinositol deficiency in patients with hyperphosphatasia mental retardation syndrome. J Biol Chem 287(9):6318–6325. doi:10.1074/jbc.M111.331090
22. Mornet E (2007) Hypophosphatasia. Orphanet J Rare Dis 2:40. doi: 10.1186/1750-1172-2-40

European Journal of Haematology

European Journal of Haematology 92 (450–453)

CASE REPORT

Paroxysmal nocturnal hemoglobinuria with copy number-neutral 6pLOH in GPI (+) but not in GPI (−) granulocytes

Yasutaka Ueda[1], Jun-ichi Nishimura[2], Yoshiko Murakami[3,4], Sachiko Kajigaya[1], Taroh Kinoshita[3,4], Yuzuru Kanakura[2], Neal S. Young[1]

[1]Hematology Branch, National Heart, Lung, and Blood Institute, National Institutes of Health, Bethesda, MD, USA; [2]Department of Hematology and Oncology, Osaka University Graduate School of Medicine, Osaka; [3]Department of Immunoregulation, Research Institute for Microbial Diseases, Osaka University, Osaka; [4]Department of Immunoglycobiology, WPI Immunology Frontier Research Centre, Osaka University, Osaka, Japan

Abstract

Paroxysmal nocturnal hemoglobinuria (PNH) is an acquired bone marrow disorder caused by expansion of a clone of hematopoietic cells lacking glycosylphosphatidylinositol (GPI)-anchored membrane proteins. Multiple lines of evidence suggest immune attack on normal hematopoietic stem cells provides a selective growth advantage to PNH clones. Recently, frequent loss of HLA alleles associated with copy number-neutral loss of heterozygosity in chromosome 6p (CN-6pLOH) in aplastic anemia (AA) patients was reported, suggesting that AA hematopoiesis 'escaped' from immune attack by loss of HLA alleles. We report here the first case of CN-6pLOH in a Japanese PNH patient only in GPI-anchored protein positive (59%) granulocytes, but not in GPI-anchored protein negative (41%) granulocytes. CN-6pLOH resulted in loss of the alleles *A*02:06-DRB1*15:01-DQB1*06:02*, which have been reported to be dominant in Japanese PNH patients. Our patient had maintained nearly normal blood count for several years. Our case supports the hypothesis that a hostile immune environment drives selection of resistant hematopoietic cell clones and indicates that clonal evolution may occur also in normal phenotype (non-PNH) cells in some cases.

Key words paroxysmal nocturnal hemoglobinuria; array comparative genomic hybridization; loss of heterozygosity; clonal evolution; bone marrow failure syndromes

Correspondence Yasutaka Ueda, Hematology Branch, NHLBI/NIH, Bldg 10-CRC, Rm 3E-5216, 9000 Rockville Pike, Bethesda, MD 20892, USA. Tel: 301-451-7132; Fax: 301-496-8396; e-mail: ueday2@nhlbi.nih.gov

Accepted for publication 15 December 2013

doi:10.1111/ejh.12253

Paroxysmal nocturnal hemoglobinuria (PNH) is a rare, life-threatening bone marrow failure syndrome, which is characterized by three major features: intravascular hemolytic anemia, bone marrow failure, and thrombosis (1). PNH is an acquired clonal disorder of the hematopoietic stem cell (HSC) caused by a somatic mutation of the X-linked phosphatidylinositol glycan class A (*PIGA*) gene in one or a few hematopoietic stem cells (2). Even healthy individuals were reported to have very small number of PNH cells (3). The mechanism of clonal expansion of PNH cells is not understood, but the close association between PNH and aplastic anemia (AA) suggests that immune-mediated attack to hematopoietic stem cells underlies the pathogenesis of the association. Some data support a model of PNH clone expansion based on autoimmunity. PNH clones were less sensitive to NK and T-cell killing due to lack of expression of stress-inducible GPI-anchored proteins ULBP1 and ULBP2 in vitro and with patients granulocytes (4, 5), and an inefficient T lymphocyte response was observed to GPI (−) cells *in vitro* and in mouse models (6). Recently, frequent loss of HLA alleles associated with copy number-neutral loss of heterozygosity of the 6p arms (CN-6pLOH) in AA patients was reported (7). Here, we describe the first case of a PNH patient with CN-6pLOH in GPI (+) granulocytes, but not in GPI (−) granulocytes.

Patient and methods

A 33-year-old male presented to hospital for mild thrombocytopenia (130×10^9/L), and PNH was diagnosed by flow

cytometry (1). The patient had not been treated for 2 years and 6 months due to lack of symptoms of anemia or thrombosis, although he had experienced hemoglobinuria several times a year since diagnosis. PNH clone sizes were 49.0% and 22.0% in granulocytes and red blood cells, respectively, at diagnosis and were 45.2% and 28.5%, respectively, 12 months after the diagnosis. LDH had remained elevated (500–600 U/L). At the time of array comparative genomic hybridization (aCGH) analysis, 24 months after the diagnosis, the proportions of GPI-negative cells were 40.9%, 25.7%, and 4.7% in granulocytes, red blood cells, and T cells, respectively. Blood count included leukocytes 3.7×10^9/L, (38.8% neutrophils, 48.0% lymphocytes, 8.7% monocytes, 0.8% eosinophils, and 0.5% basophils), hemoglobin 14.4 g/dL, MCV 101.9 fl, platelets 113×10^9/L, and reticulocyte count 112×10^9/L. LDH was elevated at 620 U/L (normal range up to 229 U/L). Informed consent was obtained from the patient in accordance with protocols approved by the Institutional Review Boards of Osaka University Hospital. Red blood cells were analyzed for GPI-anchored proteins with anti-CD55 and anti-CD59 antibodies within a CD235 positive population. Peripheral blood granulocytes (CD11b + 7AAD−) and T cells (CD3 + 7AAD−) were separated into GPI (+) and GPI (−) cells by Flaer (Pinewood Scientific Services, Victoria, BC, Canada) staining. After sorting, each cell population of granulocytes was subjected to DNA extraction with the QIAamp DNA Blood Mini kit or the QIAamp DNA Micro kit (QIAGEN, Hilden, Germany). High-resolution genome-wide DNA copy number analysis was performed with both GPI (+) and GPI (−) granulocytes using the CytoScan®HD Array (Affymetrix, Santa Clara, CA, USA). Sample processing was performed at Coriell Genotyping and Microarray Center, Coriell Institute for Medical Research (Camden, NJ, USA). Data were analyzed with Affymetrix Chromosome Analysis Suite (CHAS). For the analysis of clonal lesions, loss of heterozygosity (LOH) was called when the deletion was more than 25 Mb and involved telomeres (8). Alleles at *HLA-A*, *-B*, *-DRB1*, *-DQB1*, and *-DPB1* loci were identified by PCR and sequence-specific oligonucleotide probes (PCR-SSOP) method using the WAKFlow HLA Typing kit (Wakunaga, Hiroshima, Japan) at the HLA Foundation Laboratory (Kyoto, Japan), as described previously (9). Briefly, target DNA was PCR amplified with 5′-biotin-labeled primers that are highly specific to sequences of HLA genes. Amplified DNA was denatured and hybridized to locus-specific probes conjugated to microbeads labeled with streptavidin–phycoerythrin. The fluorescent intensity of phycoerythrin on each coded oligobead was measured by the Luminex® 100 system (Luminex, Austin, TX, USA). The data analysis was performed using the WAKFlow® Typing Software (Wakunaga). The haplotypes of six loci were inferred based on the data of haplotype frequencies of a Japanese population (701 families; $n = 2972$) estimated by direct counting method. The data are available at the Web site of the HLA Foundation Laboratory (http://hla.or.jp/haplo/haplonavi.php?type=haplo&lang=en).

Results and discussion

The Affymetrix CytoScan® HD Array contains more than 2.4 million markers for copy numbers and 750 thousand single nucleotide polymorphisms, enabling detection of high-resolution copy number, LOH detection, and breakpoint estimation across the genome. We employed the CytoScan®HD Array for aCGH analysis of submicroscopic aberrations of genomes in three Japanese PNH patients who had both GPI (+) and GPI (−) cells in granulocytes. Remarkably, CN-6pLOH was detected in a GPI (+) granulocyte population, but not in a GPI (−) granulocyte popula-

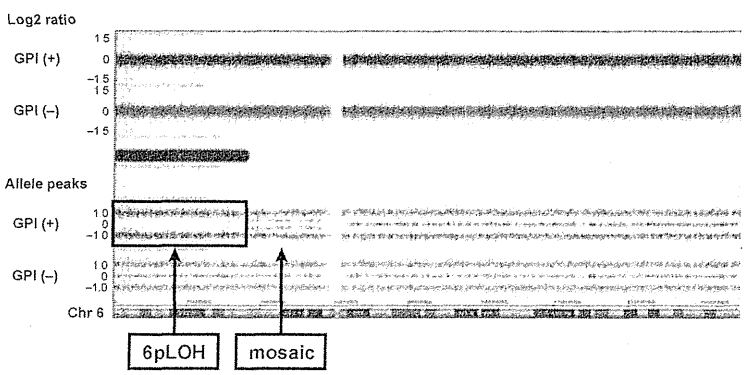

Figure 1 Acquired CN-6pLOH in GPI (+) granulocytes but not in GPI (−) granulocytes. Upper panel shows copy number status by log2 ratio: Theoretically, the log 2 ratio of normal (copy number-neutral) clones is log2 (2/2) = 0 and of single copy losses is log2 (1/2) = −1. Lower panel shows allele frequency calculated as the difference between the signals of the A allele minus B allele. Homozygous AA maps to approximately +1, and homozygous BB allele maps to approximately −1, with the heterozygote mapping to approximately 0. Single A and B allele maps to 0.5 and −0.5, respectively. Copy number was neutral in 6p arm, but loss of heterozygosity (the disappearance of the heterozygote signal) was observed with mosaicism near the centromere.

tion, in a single patient (Fig. 1). Mosaicism was observed near the centromere of 6p, suggesting there were at least two clones with CN-6pLOH in GPI (+) cells. Both of the CN-LOH covered HLA class I and class II genes (6p21.2–6p25.3 and 6p11.2–6p25.3). HLA typing of the patient by PCR-SSOP method was *A*02:06, A*26:02, B*35:01, B*40:06, C*03:03, C*08:01, DRB1*09:01, DRB1*15:01, DQB1*03:03, DQB1*06:02, DPB1*02:01, DPB1*05:01*. The haplotype of *A*02:06-B*35:01-C*03:03-DRB1*15:01-DQB1*06:02- DPB1*05:01* was lost in 80%–90% of GPI (+) granulocytes due to 6pLOH. High frequency of CN-6pLOH in AA patients was reported by a Japanese group (7), and particular alleles including *HLA-A*02:06* were dominantly missing, suggesting 6pLOH hematopoietic stem cells escape from the immune attack mediated by cytotoxic T cells (CTLs), which may recognize unknown antigens on class I HLA molecules. HLA alleles *A*02:06, DRB1*15:01,* and *DQB1*06:02* were reported to be frequent among Japanese PNH patients (10, 11), suggesting that an immunological mechanism underlies the expansion of PNH clones. Immune mechanisms have long been hypothesized for the expansion of PNH clones with some support in the literatures. PNH clones were reported to be less sensitive to NK and T-cell killing (4, 5) or CD4 + T cells (6). GPI itself was suggested to be an autoantigen recognized by GPI-specific T cells (12, 13). GPI (+) granulocytes reflect purportedly 'normal' hematopoiesis, but our previous studies showed frequent chromosomal abnormalities and apoptotic gene expression in this 'normal' population. Based on these observations, in this patient, 80% to 90% of GPI (+) granulocytes were derived from clones that might have escaped immune attack by loss of the haplotype and therefore able to maintain nearly normal hematopoiesis for several years. The PNH clone in this patient propagated without loss of HLA alleles, supporting the idea that PNH clones are less susceptible to immune attack even when they express target antigens. HLA-restricted CTLs might have led to clonal selection of GPI (+) cells in our patient, but how the PNH cells in the same patient escaped attack is unknown. 6pLOH in the GPI (−) clone could result from mitotic recombination, but it is still to be clarified if additional CN-6pLOH endows GPI (−) cells with a comparative growth advantage under HLA-restricted immune attack. Clonal evolution in both the GPI (+) and GPI (−) cells may have caused the balanced coexistence with nearly normal blood count. Further analysis would be necessary to examine whether this phenomenon is common in other PNH patients, and assessment of both clones in the patient would be needed. In conclusion, our case supports the hypothesis that a hostile immune environment drives selection of resistant hematopoietic cell clones and indicates that clonal evolution may occur also in normal phenotype (non-PNH) cells in some cases.

Acknowledgements

This research was supported by the Intramural Research Program of the NIH, the NHLBI, and in part by a Grant-in-Aid for Scientific Research from the Ministry of Education, Culture, Sports, Science and Technology of Japan. The authors thank Satoru Hayashi for excellent technical assistance.

Authorship contributions

NSY was the principal investigator and takes primary responsibility for the paper; YU, SK, and NSY designed the research; YU and SK performed the laboratory work for this study; JN, YM, and YK recruited the patients in Japan and provided vital patients samples and clinical information; TK, YK, and NSY coordinated and supervised the study; YU and NSY wrote the manuscript. All authors approved the final version of the manuscript.

Conflict of interest disclosures

The authors report no potential conflict of interest.

References

1. Parker C, Omine M, Richards S, *et al.* Diagnosis and management of paroxysmal nocturnal hemoglobinuria. *Blood* 2005;**106**:3699–709.
2. Takeda J, Miyata T, Kawagoe K, Iida Y, Endo Y, Fujita T, Takahashi M, Kitani T, Kinoshita T. Deficiency of the GPI anchor caused by a somatic mutation of the PIG-A gene in paroxysmal nocturnal hemoglobinuria. *Cell* 1993;**73**:703–11.
3. Araten DJ, Nafa K, Pakdeesuwan K, Luzzatto L. Clonal populations of hematopoietic cells with paroxysmal nocturnal hemoglobinuria genotype and phenotype are present in normal individuals. *Proc Natl Acad Sci USA* 1999;**96**:5209–14.
4. Nagakura S, Ishihara S, Dunn DE, *et al.* Decreased susceptibility of leukemic cells with PIG-A mutation to natural killer cells in vitro. *Blood* 2002;**100**:1031–7.
5. Hanaoka N, Kawaguchi T, Horikawa K, Nagakura S, Mitsuya H, Nakakuma H. Immunoselection by natural killer cells of PIGA mutant cells missing stress-inducible ULBP. *Blood* 2006;**107**:1184–91.
6. Murakami Y, Kosaka H, Maeda Y, Nishimura J, Inoue N, Ohishi K, Okabe M, Takeda J, Kinoshita T. Inefficient response of T lymphocytes to GPI-anchor-negative cells: implications for paroxysmal nocturnal hemoglobinuria. *Blood* 2002;**100**:4116–22.
7. Katagiri T, Sato-Otsubo A, Kashiwase K, *et al.* Frequent loss of HLA alleles associated with copy number-neutral 6pLOH in acquired aplastic anemia. *Blood* 2011;**118**:6601–9.
8. Maciejewski JP, Tiu RV, O'Keefe C. Application of array-based whole genome scanning technologies as a cytogenetic tool in haematological malignancies. *Br J Haematol* 2009;**146**:479–88.

9. Itoh Y, Mizuki N, Shimada T, Azuma F, Itakura M, Kashiwase K, Kikkawa E, Kulski JK, Satake M, Inoko H. High-throughput DNA typing of HLA-A, -B, -C, and -DRB1 loci by a PCR-SSOP-Luminex method in the Japanese population. *Immunogenetics* 2005;**57**:717–29.
10. Shichishima T, Okamoto M, Ikeda K, Kaneshige T, Sugiyama H, Terasawa T, Osumi K, Maruyama Y. HLA class II haplotype and quantitation of WT1 RNA in Japanese patients with paroxysmal nocturnal hemoglobinuria. *Blood* 2002;**100**:22–8.
11. Shichishima T, Noji H, Ikeda K, Akutsu K, Maruyama Y. The frequency of HLA class I alleles in Japanese patients with bone marrow failure. *Haematologica* 2006;**91**:856–7.
12. Karadimitris A, Luzzatto L. The cellular pathogenesis of paroxysmal nocturnal haemoglobinuria. *Leukemia* 2001;**15**:1148–52.
13. Gargiulo L, Papaioannou M, Sica M, *et al.* Glycosylphosphatidylinositol-specific, CD1d-restricted T cells in paroxysmal nocturnal hemoglobinuria. *Blood* 2013;**121**:2753–61.

BJ Biomolecules

Biochem. J. (2014) 463, 249–256 (Printed in Great Britain) doi:10.1042/BJ20140541

New insights into the functions of PIGF, a protein involved in the ethanolamine phosphate transfer steps of glycosylphosphatidylinositol biosynthesis

Matthew J. STOKES*, Yoshiko MURAKAMI*†, Yusuke MAEDA*†, Taroh KINOSHITA*† and Yasu S. MORITA*†[1]

*Laboratory of Immunoglycobiology, WPI Immunology Frontier Research Center, Osaka University, Osaka 565-0871, Japan
†Department of Immunoregulation, Research Institute for Microbial Diseases, Osaka University, Osaka 565-0871, Japan

PIGF is a protein involved in the ethanolamine phosphate (EtNP) transfer steps of glycosylphosphatidylinositol (GPI) biosynthesis. PIGF forms a heterodimer with either PIGG or PIGO, two enzymes that transfer an EtNP to the second or third mannoses of GPI respectively. Heterodimer formation is essential for stable and regulated expression of PIGO and PIGG, but the functional significance of PIGF remains obscure. In the present study, we show that PIGF binds to PIGO and PIGG through distinct molecular domains. Strikingly, C-terminal half of PIGF was sufficient for its binding to PIGO and PIGG and yet this truncation mutant could not complement the PIGF defective mutant cells, suggesting that heterodimer formation is not sufficient for PIGF function. Furthermore, we identified a highly conserved motif in PIGF and demonstrated that the motif is not involved in binding to PIGO or PIGG, but critical for its function. Finally, we identified a PIGF homologue from *Trypanosoma brucei* and showed that it binds specifically to the *T. brucei* PIGO homologue. These data together support the notion that PIGF plays a critical and evolutionary conserved role in the ethanolamine-phosphate transfer-step, which cannot be explained by its previously ascribed binding/stabilizing function. Potential roles of PIGF in GPI biosynthesis are discussed.

Key words: ethanolamine phosphate transferase, glycosylphosphatidylinositol, membrane protein, metabolism, PIGF, *Trypanosoma brucei*.

INTRODUCTION

Phosphatidylinositol-anchored proteins and glycans are found in evolutionarily diverse organisms including bacteria, protozoa, fungi, plants and animals. The structure of eukaryotic glycosylphosphatidylinositol (GPI) was first revealed by using a GPI-anchored variant surface glycoprotein of *Trypanosoma brucei* in 1985 [1,2]. Since then, structures of GPI-anchored proteins have been reported from many organisms and it has become clear that the core structure of protein-EtNP-6Manα1,2Manα1,6Manα1,4GlcNα1,6*myo*-inositol-phospholipid is highly conserved through the eukaryotic evolution [EtNP (ethanolamine phosphate); Man (mannose); GlcN (glucosamine)] (Figure 1). More than 20 genes involved in the GPI-anchor biosynthesis have been identified [3]. This core structure is modified by a variety of structures such as additional EtNP or mono/oligo-saccharides, but the physiological significance of various modifications in various GPI-anchored proteins remains largely unknown.

An evolutionarily conserved feature of GPI structure in mammalian and yeast cells is that an additional EtNP residue modifies both the first and second mannoses in addition to the third mannose. Phosphatidylinositol glycan anchor biosynthesis, class O (PIGO; Gpi13p in yeast) is involved in the attachment of the core EtNP on to the third mannose [4–6]. The donor of EtNP is phosphatidylethanolamine (PE) [7,8] and its EtNP moiety is transferred to GPI in a transphosphodiesterase reaction. Indeed, PIGO has conserved motifs found in phosphodiesterases and nucleotide pyrophosphatases, suggesting that it has a catalytic function. Homologues of PIGO, namely phosphatidylinositol glycan anchor biosynthesis, class N (PIGN; Mcd4p in yeast) and phosphatidylinositol glycan anchor biosynthesis, class G (PIGG; Gpi7p in yeast), mediate the transfer of EtNP to the first and second mannoses respectively [9–13]. Although the physiological significance of these additional EtNP structures are poorly understood, these steps are critical for GPI-anchor biosynthesis and trafficking. In yeast, a terpenoid lactone, YW3548, which inhibits the enzymatic activity of Mcd4p [9], blocked the addition of the third mannose, suggesting that EtNP needs to be attached to the first mannose before the third mannose transfer occurs [14]. Furthermore, mutation in the *PIGN* gene is associated with defects in forebrain development in mice and an autosomal recessive syndrome in human characterized by dysmorphic features and congenital neurological abnormalities [15–17]. *GPI7* is not an essential gene in yeast and a GPI-intermediate lacking an EtNP attachment mediated by Gpi7p can still be transferred to proteins [11,13]. Nevertheless, yeast GPI7 has been implicated in cell separation and subsequent growth of daughter cells [18]. More recently, we demonstrated in mammalian cells that the second EtNP added by PIGG is removed in the endoplasmic reticulum (ER) by a phosphodiesterase, PGAP5, soon after attachment to

Abbreviations: ALDH, acetaldehyde dehydrogenase; CHO, Chinese-hamster ovary; ER, endoplasmic reticulum; EtNP, ethanolamine phosphate; GlcN, glucosamine; GPI, glycosylphosphatidylinositol; PE, phosphatidylethanolamine; PIG, phosphatidylinositol glycan anchor biosynthesis; TM, transmembrane, WT, wild-type.

[1] To whom correspondence should be addressed at the present address: Department of Microbiology, University of Massachusetts, Amherst, MA 01003, U.S.A. (email ymorita@microbio.umass.edu).

Table 1 Primers used in the present study

Name	Forward primer sequence (5′→3′)	Reverse primer sequence (5′→3′)
PIGF-ΔN1	AAAACTGCAGGACTACAAGGACGACGATGACAAGGTCGACGAGAACTTCTCAATATTG	ATAGTTTAGCGGCCGCTTAATTGTTCTTGTATGT
PIGF-ΔN2	AAAACTGCAGCCACCATGGACTACAAGGACGACGATGACAAGGTCGACAAACCAAATACATCCTCT	ATAGTTTAGCGGCCGCTTAATTGTTCTTGTATGT
PIGF-ΔN3	AAAACTGCAGGACTACAAGGACGACGATGACAAGGTCGACTATGGAGCACCACTGATA	ATAGTTTAGCGGCCGCTTAATTGTTCTTGTATGT
PIGF-ΔC1	AAAACTGCAGCCACCATGGACTACAAGGACGACGATGACAAGGTCGACAAAGATAACGATATCAAG	ATAGTTTAGCGGCCGCTTACGTACAGGAGATGGGCCA
PIGF-ΔC2	AAAACTGCAGCCACCATGGACTACAAGGACGACGATGACAAGGTCGACAAAGATAACGATATCAAG	ATAGTTTAGCGGCCGCTTACTGGAGACTATTCTCCCA
PIGF-ΔC3	AAAACTGCAGCCACCATGGACTACAAGGACGACGATGACAAGGTCGACAAAGATAACGATATCAAG	ATAGTTTAGCGGCCGCTTATGTTTCCAATGCCAACTC
PIGF-ΔN1ΔC1	AAAACTGCAGGACTACAAGGACGACGATGACAAGGTCGACGAGAACTTCTCAATATTG	ATAGTTTAGCGGCCGCTTACGTACAGGAGATGGGCCA
TbPIGF	ACGCGTCGACGTTCTTTGGGTAGTTATTTTCTCACTCGCT	ATAGTTTAGCGGCCGCTTATTCCACCTTTTCATCAACCTTCTCTGGT
TbPIGO	CCGGAATTCCCACCATGACCTCACGCTCTGAT	CGACGCGTTGCCAGTAACGCAGC

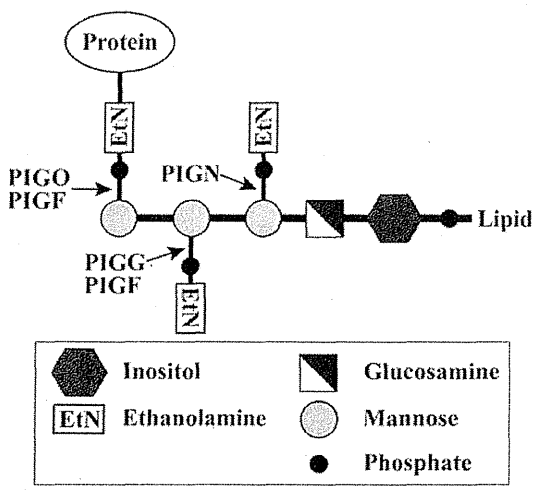

Figure 1 Structure of GPI-anchor core glycan and enzymes involved in the biosynthesis

proteins and suggested that EtNP attached to the second mannose regulates GPI-anchored protein transport in the early secretory pathway [19].

Phosphatidylinositol glycan anchor biosynthesis, class F (PIGF) is another protein involved in EtNP transfer steps of GPI biosynthesis. It is an extremely hydrophobic protein made of 219 amino acid residues in the case of human PIGF [20]. Six transmembrane (TM) domains, identified using the programs SOSUI [21] and TMHMM [22], are distributed through the entire protein. PIGF was initially identified as a protein involved in the addition of the third mannose [4]. Indeed, PIGF binds to PIGO, and PIGO quickly degrades in the absence of PIGF, indicating that PIGF is important for stable expression of PIGO [4]. Interestingly, PIGF binds not only to PIGO but also to PIGG and the stable expression of PIGG is also dependent on PIGF [10]. These observations suggested that PIGF is a critical protein that allows stable expression of the two EtNP transferases, PIGO and PIGG. Nevertheless, we know little about whether PIGF plays this stabilizing role and how the presence of PIGF is critical when co-ordination of multiple EtNP transferases is necessary. In the present paper, we provide evidence that PIGF uses distinct amino acid domains to interact with PIGO or PIGG. Furthermore, we demonstrate that PIGF plays an additional function that cannot be explained by its binding to PIGO or PIGG. Finally, whereas a protozoan parasite *T. brucei* lacks PIGG, we demonstrate the presence of a PIGF homologue, designated as TbPIGF, and its interaction with TbPIGO, indicating that evolution of PIGF is not dependent on the presence of PIGG.

EXPERIMENTAL

Cells and culturing

EL4 class F cells [20], a murine thymoma Thy-1-deficient cell-line, were grown in Dulbecco's modified Eagle's medium supplemented with 10 % FBS. Chinese-hamster ovary (CHO)-K1 cells were cultured in Ham's F12 medium supplemented with 10 % FBS.

Cloning, preparation of mutant constructs and transfection

Primer sets used to create PIGF mutants are shown in Table 1. Amplified PCR fragments were digested with PstI and NotI and ligated into pMEPyori_puro-FLAG-CD59 vector to generate PIGF proteins with an N-terminal FLAG tag [23]. PIGO and PIGG with an N-terminal GST tag were generated previously [4,10]. *TbPIGF* and *TbPIGO* genes were amplified and cloned into either pMEPyori_puro-FLAG-CD59 or pMEpyori4gGST expression vector. Site-directed mutagenesis was performed as described previously [23]. For transfection of EL4 class F cells, cells were grown to a density of 3×10^6 cells/ml, and 1×10^7 cells were electroporated with 20 μg of plasmid at 1000 μF and 250 V in 0.4 mm gap cuvette. The cells were then transferred to 10 ml of Eagle's medium containing 10 % FBS and cultured for 2 days. For CHO-K1 cells, 1×10^7 cells were electroporated with 20 μg of plasmid at 1000 μF and 250 V in 0.4 mm gap cuvette. The cells were then transferred to 10 ml of Ham's F12 medium containing 10 % FBS and cultured for 2 days.

Fluorescence staining and FACS analysis

Surface-expressed Thy-1 was stained by incubating cells with phycoerythrin-conjugated anti-CD90.2 antibody (Becton Dickinson) for 1 h on ice. Stained cells were analysed using a FACScan cytometer (Becton Dickinson).

Immunoprecipitation and Western blotting

Washed cells were resuspended in 0.8 ml of lysis buffer (50 mM Tris/HCl, pH 7.5, 150 mM NaCl, 1 % digitonin, 5 mM EDTA and protease inhibitor cocktail) and lysed for 1 h at 4 °C. The lysate was then centrifuged at 20000 *g* for 15 min to remove cell debris and the supernatant was incubated with glutathione–Sepharose 4B (GE Healthcare) or anti-FLAG M2 Affinity Gel

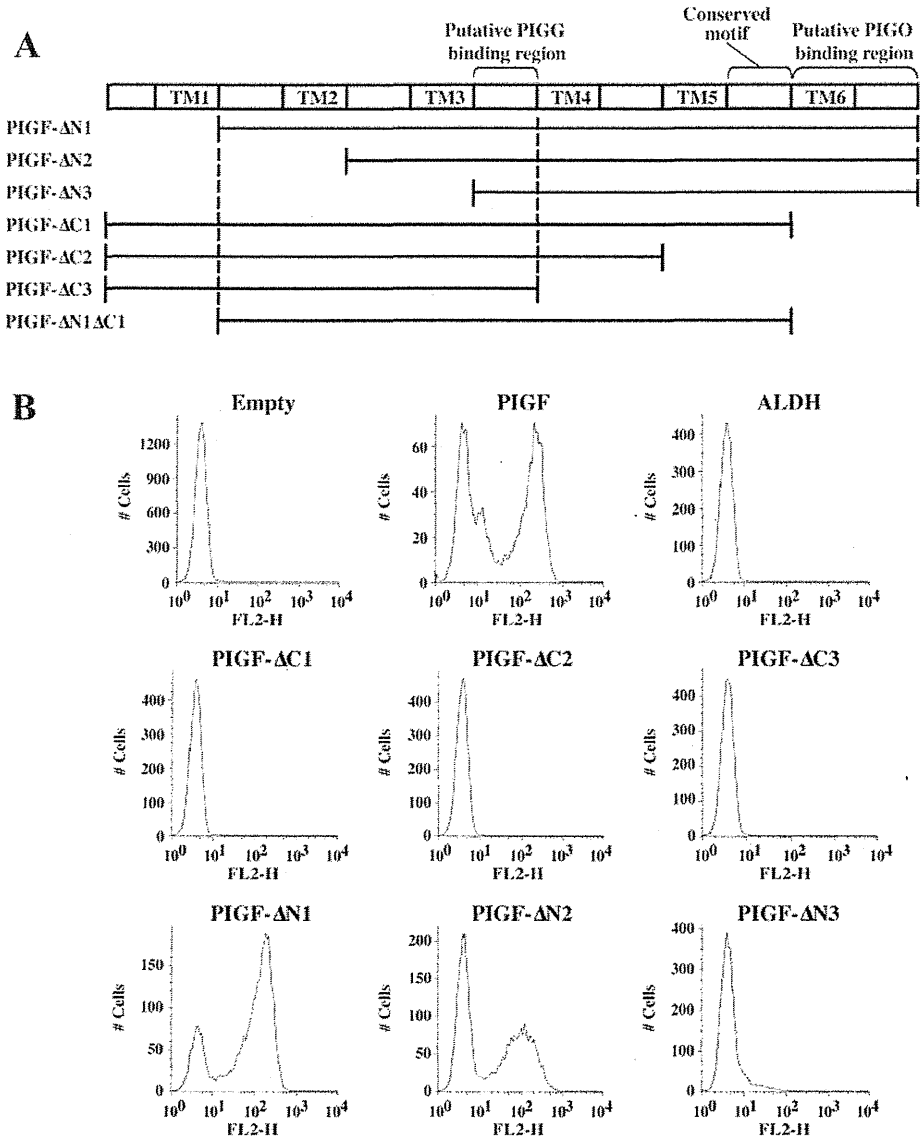

Figure 2 Complementation of PIGF-deficient cells with truncated PIGF

(**A**) Schematic representation of PIGF depicting predicted TM domains and areas of truncation in the tested constructs, binding regions and the location of the conserved motif. (**B**) EL4 class F cells were transiently transfected with the truncated PIGF constructs and tested for surface expression of Thy-1.

(Sigma). The beads were washed and bound proteins were eluted with reduced glutathione or FLAG peptide respectively. We often performed sequential pull-downs (e.g. glutathione–Sepharose pull-down and then anti-FLAG immunoprecipitation as in Figure 3) to collect unbound proteins in the initial pull-down. The eluted samples were then denatured in a sample loading buffer under reducing conditions for 1 h at 4 °C and proteins were separated by SDS/PAGE (15 % or 10–20 % gradient gel). Proteins were transferred on to PVDF membranes (Millipore) for Western blotting. Primary antibodies were mouse anti-FLAG M2 monoclonal antibody (Sigma) or goat anti-GST polyclonal antibody (GE Healthcare). For secondary antibody, horseradish peroxidase-conjugated goat anti-mouse IgG (Cell Signaling Technology) was used and the protein bands were visualized by chemiluminescence using ECL-Plus (GE Healthcare).

RESULTS

Functional domains of human PIGF

To further examine the interaction of PIGF with its binding partners, PIGO and PIGG, a series of truncated mutants were created (Figure 2A). ORFs were created to incorporate a FLAG tag at the N-terminus for constructs PIGF-ΔN2, PIGF-ΔC1, PIGF-ΔC2 and PIGF-ΔC3 and cloned in the pMEpyori vector. In order to maintain the correct orientation for constructs PIGF-ΔN1, PIGF-ΔN3 and PIGF-ΔN1ΔC1, an ORF was generated

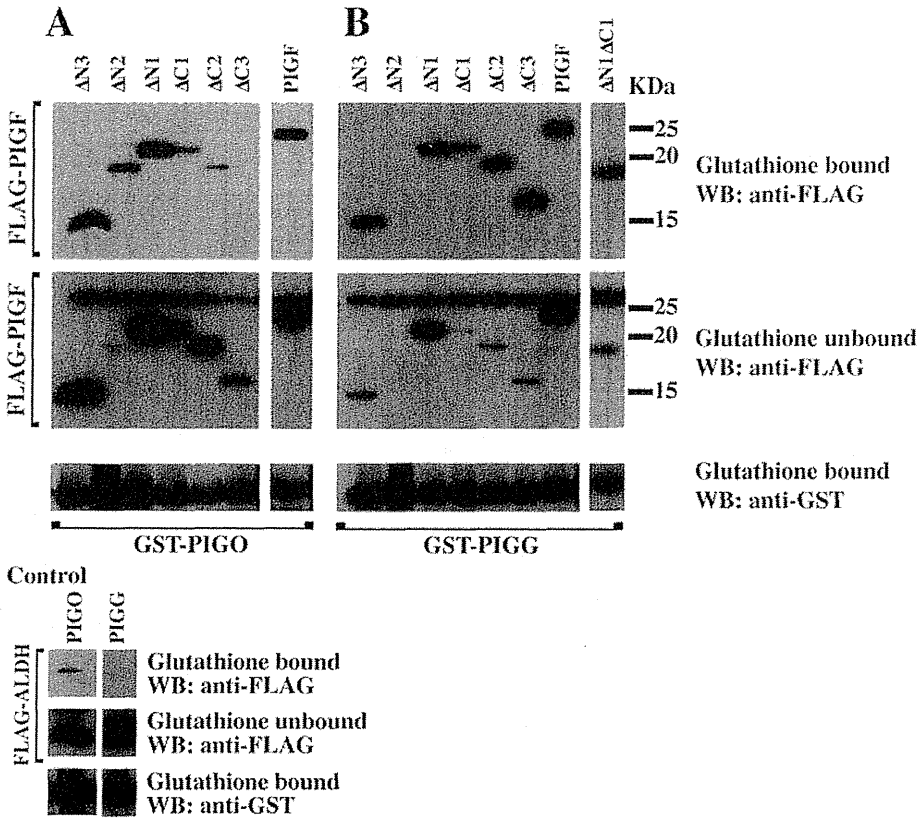

Figure 3 Binding of truncated PIGFs with PIGO and PIGG

CHO-K1 cells co-expressing WT FLAG–PIGF, truncated FLAG–PIGF or FLAG–ALDH with GST–PIGO (**A**), or GST–PIGG (**B**), were lysed in 1 % digitonin. The GST-tagged proteins in the supernatant were precipitated using glutathione beads. Unbound FLAG-tagged proteins were then precipitated with anti-FLAG–agarose. GST-tagged (bottom panels) and co-precipitated FLAG-tagged proteins (top panels) were detected by Western blot analysis using anti-GST and anti-FLAG respectively. Unbound FLAG-tagged proteins were detected using anti-FLAG antibody (middle panel). The top band constantly appearing in the middle panel is IgG light chain released during anti-FLAG immunoprecipitation.

and ligated directly into a pMEpyori containing a cleavable ER import sequence and a FLAG tag at the N-terminus [23]. To test the function of the truncated PIGF mutants, the constructs were transiently transfected into an EL4 murine thymoma cell line that lacks the surface expression of GPI-anchored proteins, such as Thy-1, due to PIGF deficiency (class F cells) [20]. Restoration of Thy-1 expression by each PIGF mutant was determined using FACS analysis (Figure 2B), and used as an indication of PIGF function. As controls, full length PIGF could restore the surface expression of Thy-1, whereas an unrelated membrane protein, acetaldehyde dehydrogenase (ALDH) had no effect on the Thy-1 expression. The removal of the C-terminal TM domain TM6 (PIGF-ΔC1) resulted in complete loss of PIGF's ability to restore Thy-1 expression in the class F cells, indicating that the C-terminal 31 amino acid residues are critical for the function or the structural integrity of PIGF. In contrast, the N-terminal two TM domains (TM1 and TM2) were not an absolute requirement for PIGF function because PIGF-ΔN1 and PIGF-ΔN2 can at least partially restore the expression of Thy-1. Further deletion (PIGF-ΔN3) abolished PIGF's ability to restore Thy-1 expression, suggesting that amino acid residues beyond position 63 carry critical residues for PIGF function. Taken together, although TM1 and TM2 are dispensable for PIGF function, the remaining C-terminal regions appear to be critical for its function.

PIGF forms heterodimers with either PIGO or PIGG and stabilizes these EtNP transferases, thereby partaking in GPI biosynthesis. We therefore wondered whether these truncated PIGF mutants lost their ability to restore Thy-1 expression because they can no longer bind to these binding partners. To test this, the truncated FLAG–PIGFs (and FLAG–ALDH as a control) were transiently co-expressed in CHO-K1 cells with GST-tagged PIGO or PIGG. The GST-tagged proteins were then immunoprecipitated with glutathione–Sepharose beads from digitonin-lysed cells and analysed for the co-immunoprecipitation of PIGF or ALDH by Western blotting. We have previously established that complexes of GPI biosynthetic enzymes are maintained in digitonin-lysed cells, but not in Nonidet P40-lysed cells [24] and successfully used ALDH, an ER-resident membrane protein as a negative control for immunoprecipitation. In the present study, we first showed that full-length PIGF binds to both PIGO and PIGG as positive controls and that ALDH binds to neither PIGO nor PIGG as negative controls (Figure 3). Figure 3(A) shows the results of co-immunoprecipitation with PIGO and indicates that the removal of the C-terminal TM domain (ΔC1, ΔC2 and ΔC3) resulted in little recovery of PIGF (upper panel). The inefficient recovery is not due to poor expression of these mutant proteins because these mutant proteins can be recovered by immunoprecipitation of unbound fractions using anti-FLAG affinity beads (lower panel). Therefore

the inability of PIGF-ΔC1, PIGF-ΔC2 and PIGF-ΔC3 to bind to PIGO is consistent with their loss of ability to restore Thy-1 expression in EL4 class F cells (see Figure 2B). These data suggest that the C-terminal TM domain is essential for PIGO binding. In contrast, the removal of the N-terminal three TM domains had no effect on PIGO binding (Figure 3A). In particular, PIGF-ΔN3 can efficiently bind to PIGO even though this construct could not restore the mutant phenotype of EL4 class F cells (see Figure 2B). These results indicate that binding of PIGF to PIGO may not be sufficient for the function of PIGF.

Because PIGF can also bind to PIGG, the inability of PIGF-ΔN3 to restore the mutant phenotype of EL4 class F cells may be attributed to its binding property to PIGG. We therefore transiently expressed the truncated FLAG–PIGFs (and FLAG–ALDH as a control) in CHO-K1 cells together with GST–PIGG. We, additionally, made a truncation mutant lacking both terminal TM domains (TM1 and TM6), designated PIGF-ΔN1ΔC1. Surprisingly, all truncated PIGFs were able to bind PIGG (Figure 3B). Because all truncated mutants contain the region between TM3 and TM4, this region may be critical for the interaction of PIGF to PIGG.

In order to clarify further the role of the C-terminal region in PIGO binding, the known PIGF amino acid sequences from various organisms were analysed. We identified a highly conserved amino acid motif consisting of the consensus PLDWxRxWQxWP (Figure 4A, red bar). To test the importance of this motif, FLAG–PIGF ORFs containing point mutations of these residues were generated and their ability to restore Thy-1 expression in class F cell was tested by FACS analysis. Only the mutations pertaining to Leu^{175} and Asp^{176} were unable to fully restore expression (Figure 4B) and point mutations W177A, Q182A, W184A and P185A were still able to restore Thy-1 expression (not shown). The importance of hydrophobicity of the leucine residue at position 175 was demonstrated by the comparison with L175K and L175A restoration effect. The effect of a positively charged lysine residue at position 175 greatly retarded Thy-1 restoration when compared with a hydrophobic alanine residue. The importance of an aspartic acid residue at position 176 was not entirely dependent on its negative charge because mutations to another negatively charged amino acid glutamic acid (D176E), positively charged amino acid lysine (D176K) or hydrophobic amino acid alanine (D176A) all showed similar reduction in surface expression of GPI-anchored proteins compared with wild-type (WT) PIGF. The combined mutation L175K/D176K had a cumulative effect and almost completely abolished PIGF's ability to restore Thy-1 expression in class F cells, indicating that these two positions are critical for the function of PIGF.

We wanted to test whether the conserved amino acids are critical for the interaction of PIGF to PIGO or PIGG. Therefore all FLAG–PIGF point mutants were co-expressed with GST–PIGO or GST–PIGG in CHO-K1 cells and immunoprecipitated using glutathione–Sepharose. All point mutants were able to bind both PIGO (Figure 4C) and PIGG (Figure 4D). Taken together, these results indicate that a conserved motif present in the C-terminal cytoplasmic loop of PIGF is functionally important, but is not involved in binding to PIGO or PIGG.

Identification of *T. brucei* PIGF and PIGO homologues

To provide insight into the evolutionary conservation of PIGF, we took advantage of the newly identified functional motif of PIGF. We used $LDW(X)_4QXWP$ as query to search the non-redundant protein sequence database at NCBI for potential PIGF homologues in other organisms. We identified a limited distribution of this motif outside of fungi, green plants and metazoans. Among these, we identified PIGF homologues in kinetoplastids (Figure 5A). The putative ORF in *T. brucei* was identified as *TbPIGF* Tb927.10.12010 (GeneID 3662199). *TbPIGF* encodes a 131-amino-acid protein with three putative TM domains. Based on amino acid sequence alignment, TbPIGF was 20.1 % identical with human PIGF.

To examine whether TbPIGF functions to bind TbPIGO, we first identified TbPIGO based on its homology with human PIGO. The putative gene *TbPIGO* (Tb927.11.5070) was cloned into a plasmid to express GST-tagged TbPIGO. This construct was transiently transfected together with a plasmid to express FLAG-tagged TbPIGF in CHO-K1 cells (Figure 5B). We then performed immunoprecipitation to examine whether TbPIGF binds to TbPIGO. We found that TbPIGF can specifically bind to TbPIGO and not to human PIGO. In contrast, human PIGF was promiscuous in that it binds to both human PIGO and TbPIGO. As a negative control, unrelated ALDH did not bind to human PIGO or TbPIGO. These data showed that TbPIGF was able to bind TbPIGO *in vivo*, further supporting a similar role for TbPIGF played in the GPI biosynthesis in *T. brucei*.

As expression and binding of TbPIGO and TbPIGF were efficient in mammalian cells, the ability of TbPIGF and TbPIGO to function in mammalian cells was tested. TbPIGF and TbPIGO were expressed alone or in combination with their mammalian binding counterpart in PIGF- and PIGO-deficient cells. The expression of these proteins failed to restore the expression of Thy-1, suggesting that they were not functional in mammalian cells (results not shown).

DISCUSSION

It was once postulated that PIGF may be an EtNP transferase [20]. However, subsequent studies demonstrated that PIGN, PIGG and PIGO are catalytic components of EtNP transferases and PIGF came to be considered as a stabilizing factor [4,10]. Our current study suggests a new additional role for PIGF, which cannot be explained by its structural role of forming heterodimers with PIGO or PIGG and stabilizing these catalytic subunits.

Two lines of evidence support our conclusion that the newly identified function of PIGF is beyond its stabilizing role. First, a truncated form of PIGF, PIGF-ΔN3, which lacks the N-terminal half of the protein, lost its functional ability to restore the surface expression of GPI-anchored proteins in a PIGF-deficient mutant (see Figure 2B), even though PIGF-ΔN3 can still bind to both PIGO and PIGG (see Figure 3). We believe that PIGF binding stabilizes PIGO and PIGG, but our data suggest that stable heterodimer formation is not sufficient for the function of PIGF. Secondly, we identified Leu^{175} and Asp^{176} as highly conserved amino acid residues critical for the function of PIGF. Double point mutation of L175K/D176K resulted in ablation of PIGF's ability to restore the surface expression of GPI-anchored proteins in a PIGF-deficient mutant (see Figure 4B). Nevertheless, the double point mutant was able to form a complex with both PIGO and PIGG, indicating again that PIGF plays a functional role that cannot be explained by binding and stabilizing PIGO and PIGG.

What is the function of PIGF? We proposed previously that the quantity of PIGF is limiting and relative activities of PIGG and PIGO are partially dictated by the availability of PIGF [10]. This scenario is based on the ability of PIGF to stably form a complex with either PIGO or PIGG, but not both, thereby controlling the relative activities of these enzymes. To consider

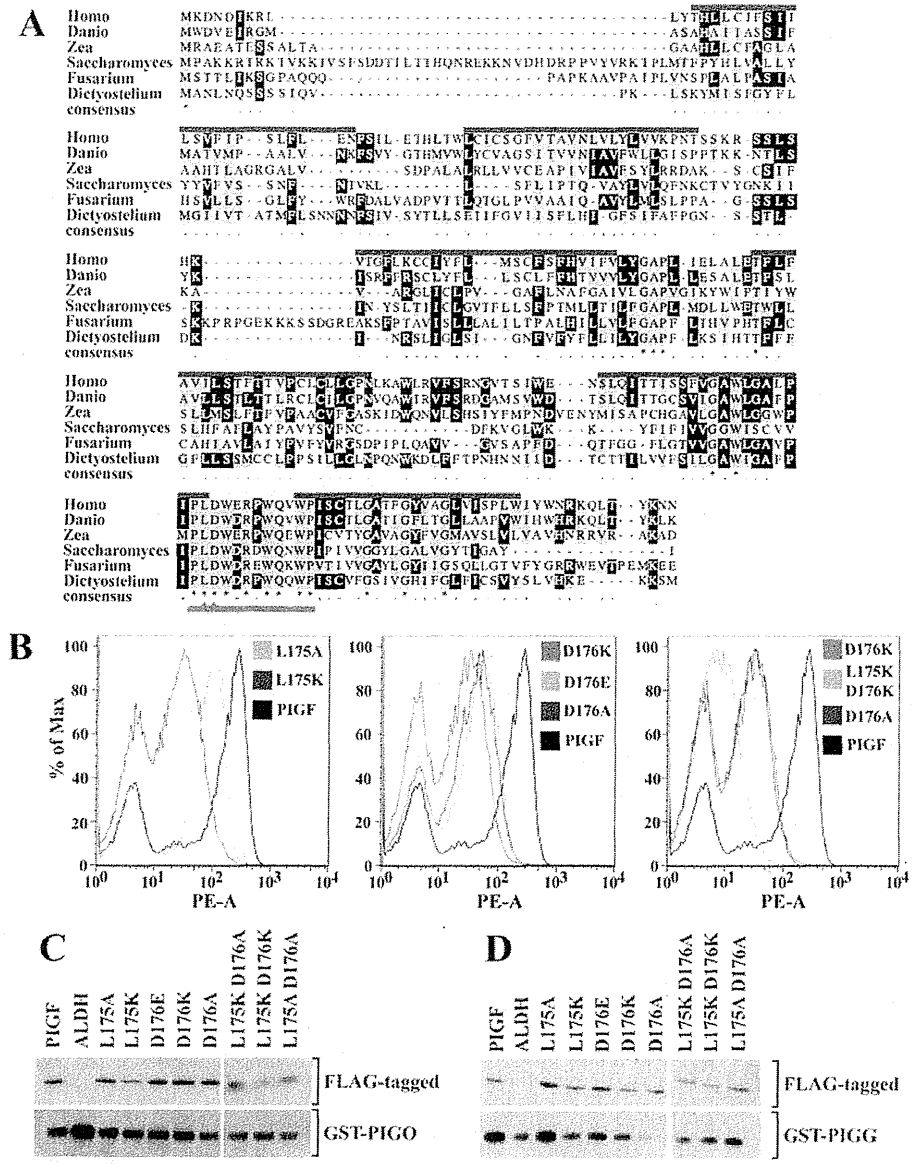

Figure 4 Evidence of functional motif in PIGF

(**A**) Alignment of amino acid sequences of PIGF homologues from *Homo sapiens* (gi|48146117), *Danio rerio* (gi|45387713), *Zea mays* (gi|525344664), *Saccharomyces cerevisiae* (gi|849212), *Fusarium pseudograminearum* (gi|408397024) and *Dictyostelium discoideum* (gi|66809485). Purple bars indicate predicted TM regions. Red bar indicates conserved motif with Leu^{175} and Asp^{176} indicated by triangles. (**B**) PIGFs containing point mutations analysed for their ability to restore Thy-1 expression in class F cells using FACS analysis. (**C** and **D**) CHO-K1 cells transiently co-expressing PIGFs containing point mutations and GST–PIGO (**C**) or GST–PIGG (**D**) were lysed in 1 % digitonin. The GST-tagged proteins in the supernatant were precipitated using glutathione beads. GST-tagged (bottom panels) and co-precipitated FLAG-tagged proteins (top panels) were detected by Western blot analysis using anti-GST and anti-FLAG respectively.

this scenario further, we took advantage of another well-studied model organism of GPI biosynthesis, *T. brucei*. *T. brucei* is a protozoan parasite responsible for African sleeping sickness in human and nagana in livestock. GPI anchors in this parasite are not modified by additional EtNP residues and there is only one protein-anchoring EtNP attached to the third mannose. As such, we could only identify a PIGO homologue in the *T. brucei* genome and homologues of PIGN and PIGG are absent. If PIGF functions solely to control the relative activities of PIGG and PIGO, there is no reason for PIGF to exist in the *T. brucei* genome. It was therefore surprising that we could identify TbPIGF and demonstrate its interaction with TbPIGO (see Figure 5). Our new data suggest that evolution of PIGF is not necessarily dependent on the presence of PIGG. Taken together with the finding that PIGF functions beyond its stabilizing roles in the formation of heterodimers, we propose that PIGF plays a more fundamental role in the biosynthesis of GPI.

There are several possibilities for the additional functions of PIGF. Since it is involved in the transfer of EtNP from PE to a GPI intermediate, it is possible that PIGF is involved in the

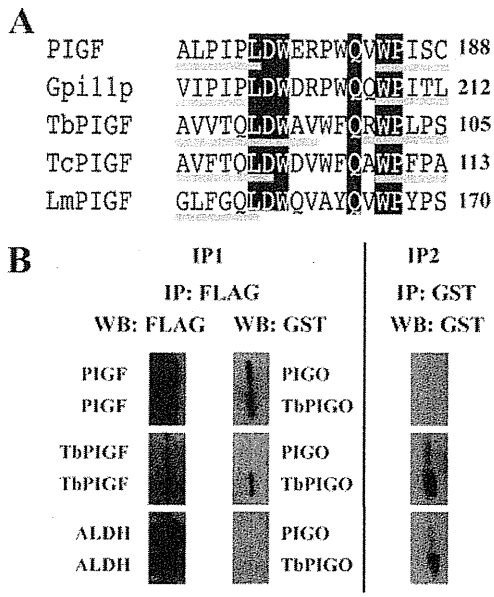

Figure 5 PIGF and PIGO homologues in *T. brucei*

(**A**) Comparison of conserved motifs from kinetoplastids with those from human (PIGF) and yeast (Gpi11p). TbPIGF (gi|71748704), TcPIGF (gi|71410645), and LmPIGF (gi|321399857: 612828-613430) indicate newly identified PIGF homologues from *T. brucei*, *Trypanosoma cruzi* and *Leishmania major*. (**B**) CHO-K1 cells transiently expressing FLAG-tagged PIGF, ALDH or TbPIGF were co-transfected with either GST-tagged TbPIGO or PIGO. Cells were lysed in 1% digitonin and the FLAG-tagged proteins in the supernatant were precipitated by anti-FLAG beads (IP1). FLAG-tagged proteins and co-precipitated GST-tagged proteins were detected by Western blot analysis using anti-GST and anti-FLAG respectively. Unbound GST-tagged proteins were immunoprecipitated by glutathione beads and detected by Western blotting using anti-GST antibody (IP2).

recruitment of these substrates to the catalytic subunit (i.e. PIGG or PIGO). We demonstrated that the aspartic acid residue in the last hydrophilic loop of PIGF is highly conserved. It is tempting to speculate that the conserved aspartic acid residue interacts with the positively charged amino group on either PE or GPI core glycan GlcN. Future studies are needed to determine its exact role in GPI biosynthesis at the molecular level.

Another focus of future research should be further analysis of heterodimer formation at the molecular level. Because both PIGF-ΔN3 and PIGF-C3 can bind to PIGG, one logical possibility is that PIGF binds to PIGG through the region between TM3 and TM4. Unfortunately, attempts to express further truncated PIGF mutants failed possibly due to the loss of protein stability. Therefore we cannot exclude an alternative possibility that two distinct binding motifs exist in PIGF for PIGG binding and one of them is sufficient for the binding of PIGF to PIGG. Whereas our current study could not pinpoint the precise amino acid residues of PIGF involved in heterodimer formation, our data demonstrate that PIGF contains two distinct binding domains: one C-terminal domain for PIGO and a second domain elsewhere for PIGG. Therefore it may be important to reconsider the possibility that PIGO, PIGG and PIGF form a heterotrimeric complex that allows efficient sequential additions of EtNP to the third and second mannose residues. Finally, we also know little about motifs in PIGO and PIGG involved in PIGF binding and more detailed studies are needed to determine the significance of interactions among these three proteins.

AUTHOR CONTRIBUTION

Matthew Stokes and Yasu Morita designed and performed experiments, analysed data and wrote the paper. Yoshiko Murakami, Yusuke Maeda and Taroh Kinoshita contributed to experimental design and data analysis.

FUNDING

This work was supported by the Ministry of Education, Culture, Sports, Science and Technology, Japan, Mizutani Foundation for Glycoscience (to T.K.) and Human Frontier Science Program Organization (to Y.S.M.).

REFERENCES

1 Ferguson, M. A. J., Low, M. G. and Cross, G. A. M. (1985) Glycosyl-*sn*-1,2-dimyristylphosphatidylinositol is covalently linked to *Trypanosoma brucei* variant surface glycoprotein. J. Biol. Chem. **260**, 14547–14555 PubMed
2 Ferguson, M. A., Homans, S. W., Dwek, R. A. and Rademacher, T. W. (1988) Glycosyl-phosphatidylinositol moiety that anchors *Trypanosoma brucei* variant surface glycoprotein to the membrane. Science **239**, 753–759 CrossRef PubMed
3 Kinoshita, T., Fujita, M. and Maeda, Y. (2008) Biosynthesis, remodelling and functions of mammalian GPI-anchored proteins: recent progress. J. Biochem. **144**, 287–294 CrossRef PubMed
4 Hong, Y., Maeda, Y., Watanabe, R., Inoue, N., Ohishi, K. and Kinoshita, T. (2000) Requirement of PIG-F and PIG-O for transferring phosphoethanolamine to the third mannose in glycosylphosphatidylinositol. J. Biol. Chem. **275**, 20911–20919 CrossRef PubMed
5 Flury, I., Benachour, A. and Conzelmann, A. (2000) YLL031c belongs to a novel family of membrane proteins involved in the transfer of ethanolaminephosphate onto the core structure of glycosylphosphatidylinositol anchors in yeast. J. Biol. Chem. **275**, 24458–24465 CrossRef PubMed
6 Taron, C. H., Wiedman, J. M., Grimme, S. J. and Orlean, P. (2000) Glycosylphosphatidylinositol biosynthesis defects in Gpi11p- and Gpi13p-deficient yeast suggest a branched pathway and implicate gpi13p in phosphoethanolamine transfer to the third mannose. Mol. Biol. Cell **11**, 1611–1630 CrossRef PubMed
7 Menon, A. K., Eppinger, M., Mayor, S. and Schwarz, R. T. (1993) Phosphatidylethanolamine is the donor of the terminal phosphoethanolamine group in trypanosome glycosylphosphatidylinositols. EMBO J. **12**, 1907–1914 PubMed
8 Menon, A. K. and Stevens, V. L. (1992) Phosphatidylethanolamine is the donor of the ethanolamine residue linking a glycosylphosphatidylinositol anchor to protein. J. Biol. Chem. **267**, 15277–15280 PubMed
9 Hong, Y., Maeda, Y., Watanabe, R., Ohishi, K., Mishkind, M., Riezman, H. and Kinoshita, T. (1999) Pig-n, a mammalian homologue of yeast Mcd4p, is involved in transferring phosphoethanolamine to the first mannose of the glycosylphosphatidylinositol. J. Biol. Chem. **274**, 35099–35106 CrossRef PubMed
10 Shishioh, N., Hong, Y., Ohishi, K., Ashida, H., Maeda, Y. and Kinoshita, T. (2005) GPI7 is the second partner of PIG-F and involved in modification of glycosylphosphatidylinositol. J. Biol. Chem. **280**, 9728–9734 CrossRef PubMed
11 Benachour, A., Sipos, G., Flury, I., Reggiori, F., Canivenc-Gansel, E., Vionnet, C., Conzelmann, A. and Benghezal, M. (1999) Deletion of GPI7, a yeast gene required for addition of a side chain to the glycosylphosphatidylinositol (GPI) core structure, affects GPI protein transport, remodeling, and cell wall integrity. J. Biol. Chem. **274**, 15251–15261 CrossRef PubMed
12 Gaynor, E. C., Mondésert, G., Grimme, S. J., Reed, S. I., Orlean, P. and Emr, S. D. (1999) MCD4 encodes a conserved endoplasmic reticulum membrane protein essential for glycosylphosphatidylinositol anchor synthesis in yeast. Mol. Biol. Cell **10**, 627–648 CrossRef PubMed
13 Imhof, I., Flury, I., Vionnet, C., Roubaty, C., Egger, D. and Conzelmann, A. (2004) Glycosylphosphatidylinositol (GPI) proteins of *Saccharomyces cerevisiae* contain ethanolamine phosphate groups on the α1,4-linked mannose of the GPI anchor. J. Biol. Chem. **279**, 19614–19627 CrossRef PubMed
14 Sütterlin, C., Horvath, A., Gerold, P., Schwarz, R. T., Wang, Y., Dreyfuss, M. and Riezman, H. (1997) Identification of a species-specific inhibitor of glycosylphosphatidylinositol synthesis. EMBO J. **16**, 6374–6383 CrossRef PubMed
15 Maydan, G., Noyman, I., Har-Zahav, A., Neriah, Z. B., Pasmanik-Chor, M., Yeheskel, A., Albin-Kaplanski, A., Maya, I., Magal, N., Birk, E. et al. (2011) Multiple congenital anomalies-hypotonia-seizures syndrome is caused by a mutation in PIGN. J. Med. Genet. **48**, 383–389 CrossRef PubMed
16 McKean, D. M. and Niswander, L. (2012) Defects in GPI biosynthesis perturb cripto signaling during forebrain development in two new mouse models of holoprosencephaly. Biol. Open **1**, 874–883 CrossRef PubMed

17 Ohba, C., Okamoto, N., Murakami, Y., Suzuki, Y., Tsurusaki, Y., Nakashima, M., Miyake, N., Tanaka, F., Kinoshita, T., Matsumoto, N. and Saitsu, H. (2014) PIGN mutations cause congenital anomalies, developmental delay, hypotonia, epilepsy, and progressive cerebellar atrophy. Neurogenetics **15**, 85–92 CrossRef PubMed
18 Fujita, M., Yoko-o, T., Okamoto, M. and Jigami, Y. (2004) GPI7 involved in glycosylphosphatidylinositol biosynthesis is essential for yeast cell separation. J. Biol. Chem. **279**, 51869–51879 CrossRef PubMed
19 Fujita, M., Maeda, Y., Ra, M., Yamaguchi, Y., Taguchi, R. and Kinoshita, T. (2009) GPI glycan remodeling by PGAP5 regulates transport of GPI-anchored proteins from the ER to the Golgi. Cell **139**, 352–365 CrossRef PubMed
20 Inoue, N., Kinoshita, T., Orii, T. and Takeda, J. (1993) Cloning of a human gene, PIG-F, a component of glycosylphosphatidylinositol anchor biosynthesis, by a novel expression cloning strategy. J. Biol. Chem. **268**, 6882–6885 PubMed
21 Hirokawa, T., Boon-Chieng, S. and Mitaku, S. (1998) SOSUI: classification and secondary structure prediction system for membrane proteins. Bioinformatics **14**, 378–379 CrossRef PubMed
22 Sonnhammer, E. L., von Heijne, G. and Krogh, A. (1998) A hidden Markov model for predicting transmembrane helices in protein sequence. Proc. Int. Conf. Intell. Syst. Mol. Biol. **6**, 175–182 PubMed
23 Hong, Y., Ohishi, K., Inoue, N., Kang, J. Y., Shime, H., Horiguchi, Y., van der Goot, F. G., Sugimoto, N. and Kinoshita, T. (2002) Requirement of N-glycan on GPI-anchored proteins for efficient binding of aerolysin but not *Clostridium septicum* alpha-toxin. EMBO J. **21**, 5047–5056 CrossRef PubMed
24 Watanabe, R., Kinoshita, T., Masaki, R., Yamamoto, A., Takeda, J. and Inoue, N. (1996) PIG-A and PIG-H, which participate in glycosylphosphatidylinositol anchor biosynthesis, form a protein complex in the endoplasmic reticulum. J. Biol. Chem. **271**, 26868–26875 CrossRef PubMed

Received 28 April 2014/25 July 2014; accepted 30 July 2014
Published as BJ Immediate Publication 30 July 2014, doi:10.1042/BJ20140541

RESEARCH ARTICLE

AMERICAN JOURNAL OF
medical genetics

Mutations in *PIGL* in a patient with Mabry syndrome

Ikuma Fujiwara,[1] Yoshiko Murakami,[2] Tetsuya Niihori,[3] Junko Kanno,[1] Akiko Hakoda,[1] Osamu Sakamoto,[1] Nobuhiko Okamoto,[4] Ryo Funayama,[5] Takeshi Nagashima,[5] Keiko Nakayama,[5] Taroh Kinoshita,[2] Shigeo Kure,[1] Yoichi Matsubara,[3,6] and Yoko Aoki[3]*

[1]Department of Pediatrics, Tohoku University School of Medicine, Sendai, Japan

[2]WPI Immunology Frontier Research Center and Research Institute for Microbial Diseases, Osaka University, Osaka, Japan

[3]Department of Medical Genetics, Tohoku University School of Medicine, Sendai, Japan

[4]Department of Medical Genetics, Osaka Medical Center and Research Institute for Maternal and Child Health, Izumi, Japan

[5]Division of Cell Proliferation, United Centers for Advanced Research and Translational Medicine, Tohoku University Graduate School of Medicine, Sendai, Japan

[6]National Research Institute for Child Health and Development, Tokyo, Japan

Manuscript Received: 10 June 2014; Manuscript Accepted: 8 December 2014

Mabry syndrome, hyperphosphatasia mental retardation syndrome (HPMRS), is an autosomal recessive disease characterized by increased serum levels of alkaline phosphatase (ALP), severe developmental delay, intellectual disability, and seizures. Recent studies have revealed mutations in *PIGV*, *PIGW*, *PIGO*, *PGAP2*, and *PGAP3* (genes that encode molecules of the glycosylphosphatidylinositol (GPI)-anchor biosynthesis pathway) in patients with HPMRS. We performed whole-exome sequencing of a patient with severe intellectual disability, distinctive facial appearance, fragile nails, and persistent increased serum levels of ALP. The result revealed a compound heterozygote with a 13-bp deletion in exon 1 (c.36_48del) and a two-base deletion in exon 2 (c.254_255del) in phosphatidylinositol glycan anchor, class L (*PIGL*) that caused frameshifts resulting in premature terminations. The 13-bp deletion was inherited from the father, and the two-base deletion was inherited from the mother. Expressing c.36_48del or c.254_255del cDNA with an HA-tag at the C- or N-terminus in *PIGL*-deficient CHO cells only partially restored the surface expression of GPI-anchored proteins (GPI-APs). Non-synonymous changes or frameshift mutations in *PIGL* have been identified in patients with CHIME syndrome, a rare autosomal recessive disorder characterized by colobomas, congenital heart defects, early onset migratory ichthyosiform dermatosis, intellectual disability, and ear abnormalities. Our patient did not have colobomas, congenital heart defects, or early onset migratory ichthyosiform dermatosis and hence was diagnosed with HPMRS, and not CHIME syndrome. These results suggest that frameshift mutations that result in premature termination in *PIGL* cause a phenotype that is consistent with HPMRS.

Key words: glycosylphosphatidylinositol anchor; Mabry syndrome; hyperphosphatasia mental retardation syndrome; genetic testing

How to Cite this Article:
Fujiwara I, Murakami Y, Niihori T, Kanno J, Hakoda A, Sakamoto O, Okamoto N, Funayama R, Nagashima T, Nakayama K, Kinoshita T, Kure S, Matsubara Y, Aoki Y. 2015. Mutations in *PIGL* in a patient with Mabry syndrome.
Am J Med Genet Part A. 9999:1–9.

INTRODUCTION

In 1970, Mabry et al. reported three siblings with increased serum levels of alkaline phosphatase (ALP), severe developmental delay, intellectual disability, and seizures [Mabry et al., 1970]. Subsequently, a condition displaying the aforementioned symptoms was referred to as hyperphosphatasia with mental retardation (HPMR) syndrome or Mabry syndrome [Krawitz et al., 2010]. Other clinical features included distinctive facial features such as hypertelorism, a

Conflict of interest: none.
Grant sponsor: Biomedical Research Core of Tohoku University Graduate School of Medicine; Grant sponsor: Ministry of Health, Labor and Welfare of Japan; Grant sponsor: Japan Society for the Promotion of Science; Grant numbers: C: 25461535, C: 23590363; Grant sponsor: Takeda Science Foundation; Grant sponsor: Ministry of Education, Culture, Sports, Science, and Technology of Japan; Grant number: 25129705.
*Correspondence to:
Yoko Aoki, M.D., Ph.D, Department of Medical Genetics, Tohoku University School of Medicine, 1-1 Seiryo-machi, Sendai 980-8574, Japan. E-mail: aokiy@med.tohoku.ac.jp
Article first published online in Wiley Online Library (wileyonlinelibrary.com): 00 Month 2015
DOI 10.1002/ajmg.a.36987

broad nasal bridge, long palpebral fissures, and a tented mouth, as well as some degree of brachytelephalangy [Horn et al., 2011]. Variable neurological abnormalities, including seizures and muscular hypotonia, were also associated with this condition. Extensive biochemical analysis showed that hyperphosphatasia was unlikely to be the result of increased activity of osteoblastic cells or hepatobiliary dysfunction, and the causes of HPMRS were unknown [Kruse et al., 1988].

In 2010, Krawitz et al. performed whole-exome sequencing of three siblings with HPMRS (OMIM 239300) and identified homozygous or compound heterozygous mutations in *PIGV* in a total of six families with HPMRS [Krawitz et al., 2010]. *PIGV* encodes a molecule that acts as the second mannosyltransferase in the glycosylphosphatidylinositol (GPI) anchor biosynthesis pathway. Subsequently, mutations in *PIGO, PGAP2, PGAP3*, and *PIGW*, which are also involved in GPI biosynthesis, have been identified in individuals with HPMRS (OMIM 614749, OMIM 614207, OMIM 615716, and OMIM 610275, respectively) [Krawitz et al., 2012, 2013; Hansen et al., 2013; Chiyonobu et al., 2014; Howard et al., 2014]. In this study, we performed whole-exome sequencing of a family with HPMRS but without mutations in *PIGV* and *PIGO* and identified compound heterozygous mutations in *PIGL*.

MATERIAL AND METHODS

Exome Sequencing

DNA was extracted using a standard protocol from blood samples of an affected female and her parents. Control DNA was obtained from 192 healthy Japanese individuals. This study was approved by the Ethics Committee of Tohoku University School of Medicine. We obtained informed consent and specific consent for photographs from the parents of the affected individual.

Exome sequencing was conducted on an individual with HPMRS. Targeted enrichment was performed using the SureSelect Human All Exon V2 kit. Exon-enriched DNA libraries were sequenced on the Illumina Hiseq 2000 for 101 bp. Burrows-Wheeler Aligner (BWA) was used to align the sequence reads to the human genome (hg19); all parameters of BWA were kept at the default settings. Following removal of duplicates from the alignments, realignment around known indels, recalibration, and SNP/indel calling were performed with Genome Analysis Toolkit (GATK, 1.5) [McKenna et al., 2010]. ANNOVAR was used for the annotation against the RefSeq database and dbSNP [Wang et al., 2010].

Sanger Sequencing

Each exon with flanking intronic sequences in *PIGV, PIGO, PIGN, PIGB*, and *PIGL* was amplified with primers based on GenBank sequences (NM_017837.2, NM_152850.3, NM_176787.4, NM_004855.4, and NM_004278.3, respectively). The M13 reverse or forward sequence was added to the 5′ end of the polymerase chain reaction (PCR) primers for use as sequencing primers. PCR was performed in 15 μl of solution containing 67 mM Tris–HCl (pH 8.8), 6.7 mM $MgCl_2$, 17 mM NH_4SO_4, 6.7 μM EDTA, 10 mM β-ME, 1.5 mM dNTPs, 10% (v/v) DMSO, 1 μM of each primer, 25 ng genomic DNA and 1 U of Taq DNA polymerase. The reaction consisted of 37 cycles of denaturation at 94°C for 20 sec, annealing at the indicated temperature for 30 sec and extension at 72°C for 30 sec. PCR products were purified using MultiScreen PCR plates (Millipore, Billerica, MA). The purified products were sequenced on an ABI 3500xL Genetic Analyzer (Applied Biosystems, Foster City, CA).

For subcloning, PCR products of exon 1 and 2 in *PIGL* were subcloned using a pTOPO TA cloning kit (Invitrogen, Carlsbad, CA) and transformed in TOP10F competent cells (Invitrogen). Plasmids were purified from each colony and sequenced.

Flow Cytometry

Surface expression of GPI-anchored proteins (GPI-APs) of granulocytes was determined by staining cells with PE-conjugated mouse anti-human CD59 (H19), anti-human DAF (IA10), anti-human CD24 (ML5), anti-human CD16 (3G8) antibodies, each isotype IgG (BD Biosciences, Franklin Lakes, NJ) and Alexa 488-conjugated inactivated aerolysin (FLAER; Protox Biotech, Canada). CD59, DAF, CD24, and CD16 are GPI-APs and FLAER binds to surface GPI-APs. The surface expression was then analyzed using a flow cytometer (Canto II; BD Biosciences) and FlowJo software (Tommy Digital, Inc., Tokyo, Japan).

Functional Analysis

PIGL-deficient CHO cells (M2S2) [Nakamura et al., 1997] were transiently transfected with *PIGL* cDNA that was driven by the strong SRα promoter (pME hPIGL-HA or pME HA-hPIGL). Two days later, cells were stained with anti-CD59, anti-DAF and FLAER and analyzed by flow cytometry. Lysates were separated using SDS–PAGE and Western blotting was performed.

RESULTS

Clinical Report

The patient was the first child of healthy and non-consanguineous Japanese parents. She was born at 33 weeks and 3 days of gestation by caesarean because of maternal infection. Her weight and height at birth were 2,510 g and 51 cm, respectively. She was treated with oxygen inhalation for several days because of transient tachypnea. She was suspected as having Beckwith–Wiedemann syndrome because of hypotonia, a large tongue, separation of the rectus abdominis muscle, and coarse facial features.

At 4 months of age, the patient's serum levels of ALP were found to be extremely high at 4,394 IU/L (Normal, 395–1,289 IU/L) and she was referred to our hospital. A radiograph of her hands showed a slight delay of bone maturation and slight dilation of the ulnar metaphysis. Alpha D3 administration was started at 5 months and ended at 1 year and 8 months of age. Laboratory investigations for inborn errors of metabolism, including toluidine blue staining in a urine sample, glycosaminoglycan in the urine, and lysosome enzymes, were normal. Karyotyping analysis on cultured leukocytes and subtelomere MLPA, FISH for 17p11.2 detecting Smith–Magenis syndrome, and array CGH analysis were all normal.

Twitching of the extremities with epileptic discharge on EEG started at 4 months of age and required anti-convulsant therapy. Brain CT and MRI showed dilatation of the bilateral lateral ven-

tricles, third and fourth ventricles and sub-arachnoid space, as well as hypoplasia of the cerebellar vermis. She was suspected as having mild deafness (right: 30 dB and left 45 dB).

At 1 year and 10 months, her weight and height were 7.9 kg (−2 SD) and 80 cm (−1 SD), respectively. Her craniofacial features included midface hypoplasia, hypertelorism, long palpebral fissures, strabismus, depressed nasal bridge, anteverted nostrils, tented upper lip vermilion, full cheeks, a high palate, and ear anomalies (Fig. 1A). Teeth eruption was not observed. In the extremities, the 2nd and 3rd digits were overlapping. The terminal phalanges of the hands and feet were short with hypoplastic nails. Her development was as follows: head control at 5 months, crawling at 1 year and 7 months, sitting at 2 year and 3 months, and walking while holding onto something at 2 years and 7 months. At 3 years and 6 months, she was unable to walk independently, and speech development was markedly delayed. ALP remained persistently elevated (3,000–4,500 U/L, Fig. 1B).

Molecular and Biochemical Analysis

Mutation screening for genes in GPI biosynthesis showed that no mutations were identifiable by Sanger sequencing analysis in any exons coding for *PIGV, PIGO, PIGN,* and *PIGB.* We then performed exome sequencing with a sample from the proband. Using the sequencing analysis pipeline from BWA and GATK, we identified approximately 8,883 nonsynonymous, nonsense, splicing site variations, coding insertions, and/or deletions (indels) per individual. Filtering steps using variant databases (dbSNP132, the 1,000 Genome Project database and ESP 5,400) resulted in the identification of 216 variants. Two frameshift mutations in *PIGL* (c.36_48del [p.Leu13Alafs*11] and c.254_255del [p.Glu86Aspfs*2]) were detected as variants in genes that participate in the GPI-anchor biosynthesis (hsa00563) and the GPI-anchor biosynthesis (hsa00563)/metabolic pathway (hsa00110) in KEGG pathway, respectively. Sanger sequencing validated the heterozygous state of the two variants in *PIGL* (Fig. 2A). Two variants resulted in a premature termination and it was assumed that truncated proteins were produced (Fig. 2B).

Subcloning of PCR products of exons 1 and 2 from parental samples followed by sequencing showed that the father was heterozygous for c.36_48del and the mother was heterozygous for c.254_255del in *PIGL,* thus confirming the compound heterozygosity in the affected individual (Fig. 2A).

The c.36_48del and c.254_255del in *PIGL* were not reported in dbSNP132, the 1,000 Genome Project database or in ESP 5,400. c.254_255del, and not c.36_48del, was reported in one in 1,000 Japanese exomes (http://www.genome.med.kyoto-u.ac.jp /SnpDB/) and identified in 1 in 192 of our in-house Japanese controls in a hetrozygous manner, suggesting that c.254_255del could be identified at a frequency of 1:200–1:1000 in Japanese people.

These genomic analyses suggested that the patient has *PIGL*-deficiency, which is one of the inherited GPI deficiencies. More than 100 mammalian proteins are modified by a GPI anchor at their C terminus [Krawitz et al., 2010]. The expression of GPI-APs have been decreased in other inherited GPI deficiencies [Maydan et al., 2011; Chiyonobu et al., 2014; Howard et al., 2014]. To examine if the GPI-APs decreased in cells from our patient, peripheral blood cells were analyzed by flow cytometry. Surface expression of various GPI-APs on the granulocytes from the patient (Fig. 3, thick lines) was severely decreased (2% of the control in CD16 expression) compared with that from the normal samples (dotted lines).

PIGL-deficient CHO cells (M2S2) [Nakamura et al., 1997] were transiently transfected with wild type (Fig. 4, dotted line),

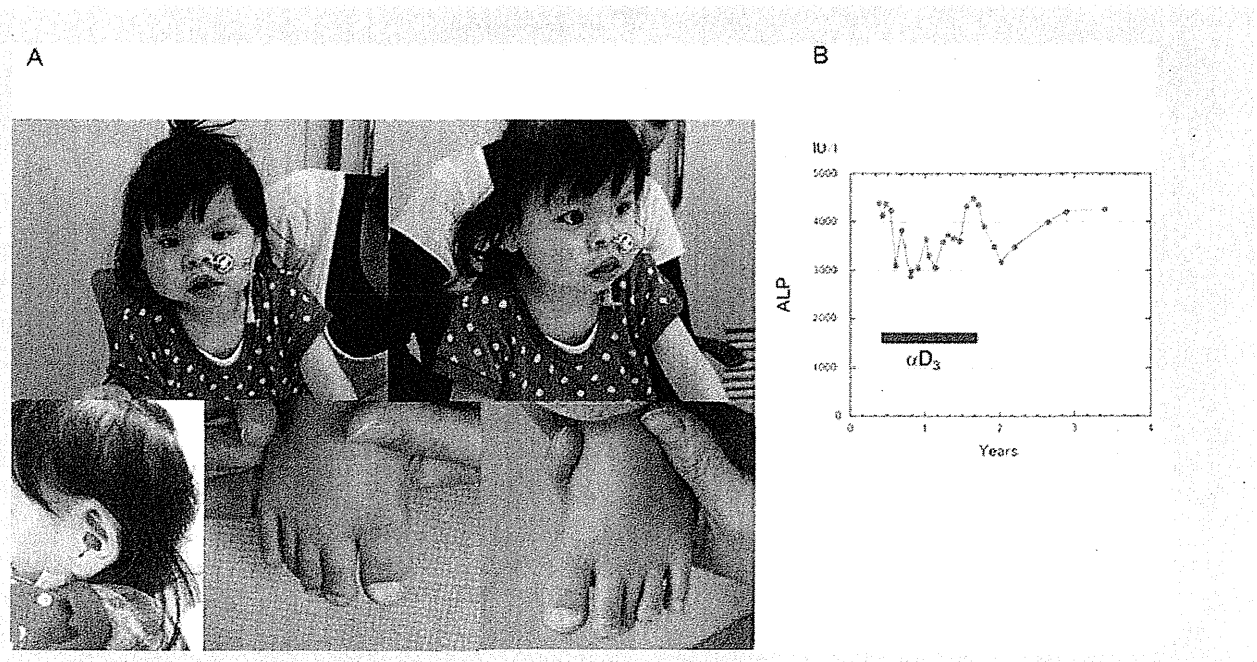

FIG. 1. Clinical manifestation of the proband. A: Photos of the girl at 2 years and 7 months of age. B: Serum levels of ALP in the patient.

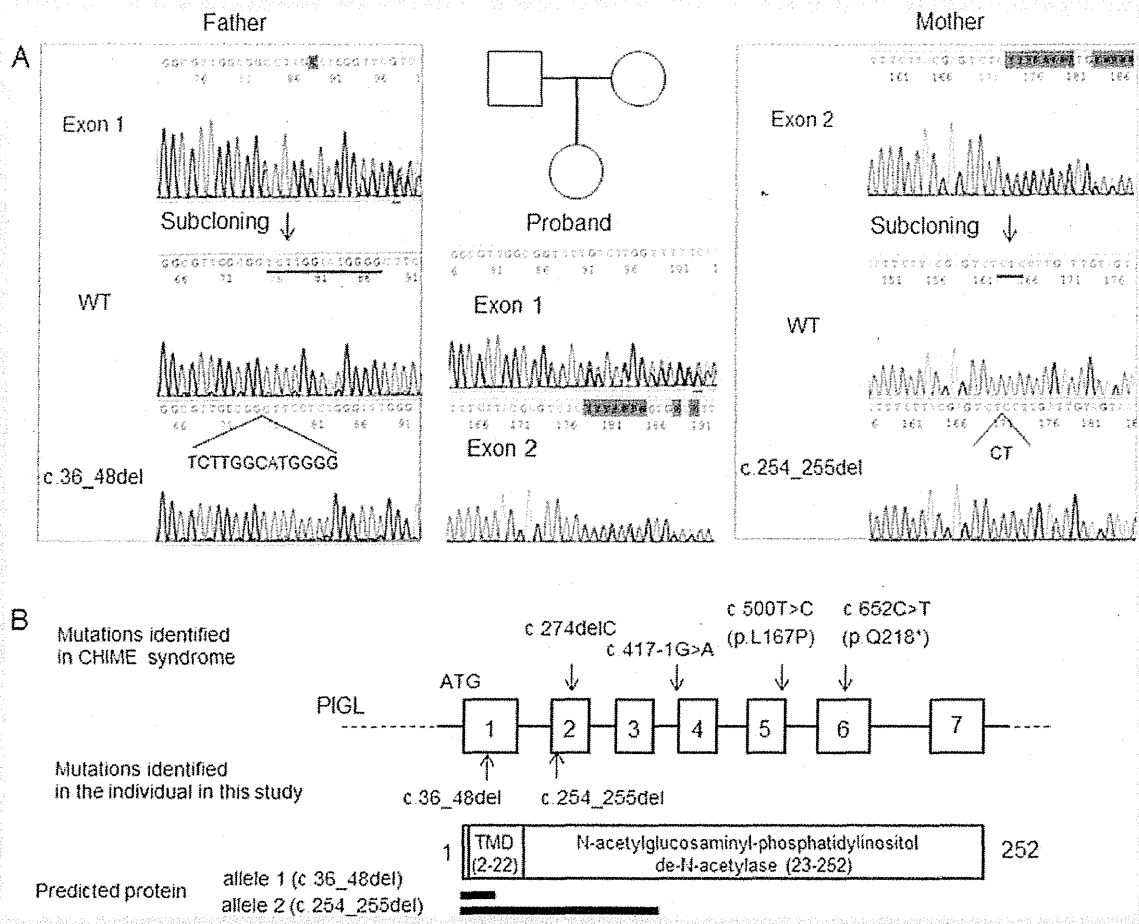

FIG. 2. Sanger sequencing of the family. A: Mutation analysis of the individual and her parents. B: The genomic structure of *PIGL* and mutations identified in CHIME syndrome and this study.

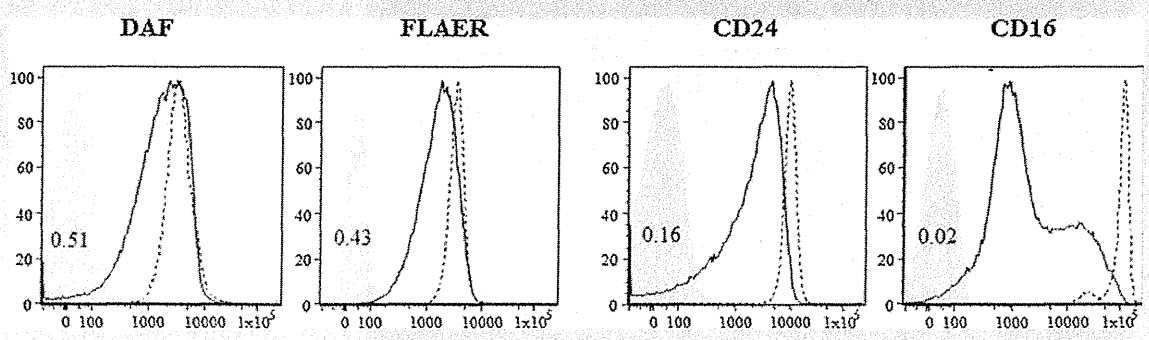

FIG. 3. Flow cytometry of granulocytes. Surface expression of various GPI-APs on the granulocytes from the patient (thick lines) was severely decreased compared with that from the normal samples (dotted lines). Light shadows are isotype controls. The value of the mean fluorescent intensity of each sample against normal is shown in each panel.

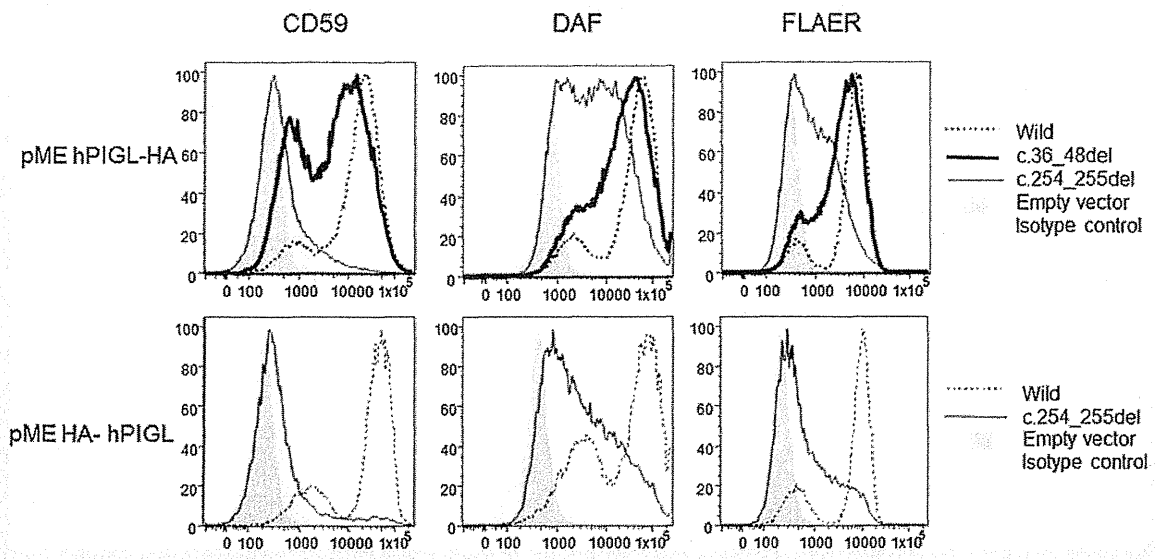

FIG. 4. PIGL-deficient CHO cells (M2S2) [Nakamura et al., 1997] were transiently transfected with wild type (dotted line), the c.36_48del mutant (thick line), or the c.254_255del mutant (thin line) PIGL cDNA that was driven by the strong SRα promoter (pME hPIGL-HA or pME HA-hPIGL) with an HA-tag at the C-(upper panels) or N-terminus (lower panels). Two days later, cells were stained with anti-CD59, anti-DAF and FLAER and analyzed by flow cytometry. The gray shadow denotes empty vector transfections; light gray shadows are isotype controls.

c.36_48del mutant (thick line) or c.254_255del mutant (thin line) *PIGL* cDNA with an HA-tag at the C-terminus (upper panels) or at the N-terminus (lower panels). Both mutants could only partially restore the surface expression of GPI-APs. The activity of the c.254_255del mutant was severely affected, and the N-terminal tagged construct had almost no activity. These results suggested that the remaining activity was not due to the truncated proteins. Faint bands (* and **) could be detected in the lysate of C-terminally tagged c.36_48 mutant transfected cells (Fig. 5A), which corresponded to the isoforms starting at the downstream methionines (2 and 3 of Fig. 5B) that showed residual PIGL activity. No band could be detected from the lysate of the c.256_255 mutant tagged at either terminus (data not shown).

DISCUSSION

We report on the case of a girl with distinctive facial features, severe intellectual disability, and persistent increased serum levels of ALP who was diagnosed with HPMRS. Whole-exome sequencing identified two frameshift mutations in *PIGL*, which were inherited from the father and mother, suggesting that *PIGL* mutations are responsible for HPMRS.

Many eukaryotic cell surface proteins are bound to the cell membrane by a GPI-anchor. More than 20 different gene products are involved in GPI biosynthesis [Fujita and Kinoshita 2012]. Recent studies revealed that genetic defects in various components of the GPI-anchor biosynthesis pathway cause inherited GPI deficiencies. Somatic mutations in *PIGA* in hematopoietic stem cells cause paroxysmal nocturnal hemoglobinuria [Ware et al., 1994]. A promoter mutation in *PIGM* causes portal venous thrombosis and absence seizures [Almeida et al., 2006]. Germline mutations in *PIGN* and *PIGA* cause congenital anomalies with hypotonia and seizures [Maydan et al., 2011; Johnston et al., 2012]. Germline mutations in *PIGV*, *PIGO*, *PGAP2*, *PGAP3*, and *PIGW* have been identified in individuals with HPMRS [Krawitz et al., 2010, 2012, 2013; Chiyonobu et al., 2014; Howard et al., 2014]. Recently, mutations in *PIGT* have been identified in a family with intellectual disability [Kvarnung et al., 2013]. Thus, the clinical spectrum of disorders caused by the GPI-anchor deficiency has expanded.

PIGL encodes a 252 amino acid endoplasmic reticulum (ER) protein, located on the ER membrane with one transmembrane region and most of the protein located on the cytoplasmic side [Nakamura et al., 1997]. PIGL is involved in the second step of GPI biosynthesis, which is de-N-acetylation of N-acetylglucosaminyl-phosphatidylinositol (GlcNAc-PI). Following de-N-acetylation, glucosaminyl-phosphatidylinositol (GlcN-PI) flips to the luminal side of ER where GlcN-PI undergoes further extensions followed by its transfer to acceptor proteins [Nakamura et al., 1997; Watanabe et al., 1999]. Mutations in *PIGL* have been identified in CHIME syndrome, an autosomal recessive disorder characterized by colobomas, congenital heart defects, early onset migratory ichthyosiform dermatosis, intellectual disability, and ear anomalies, including conductive hearing loss [Ng et al., 2012]. Our patient manifested severe intellectual disability, seizures, ear anomalies, and feeding difficulties, which overlapped with symptoms of CHIME syndrome [Ng et al., 2012]. However, our patient did not have colobomas, congenital heart defects, early onset migratory ichthyosiform, or genitourinary abnormalities. Inherited GPI

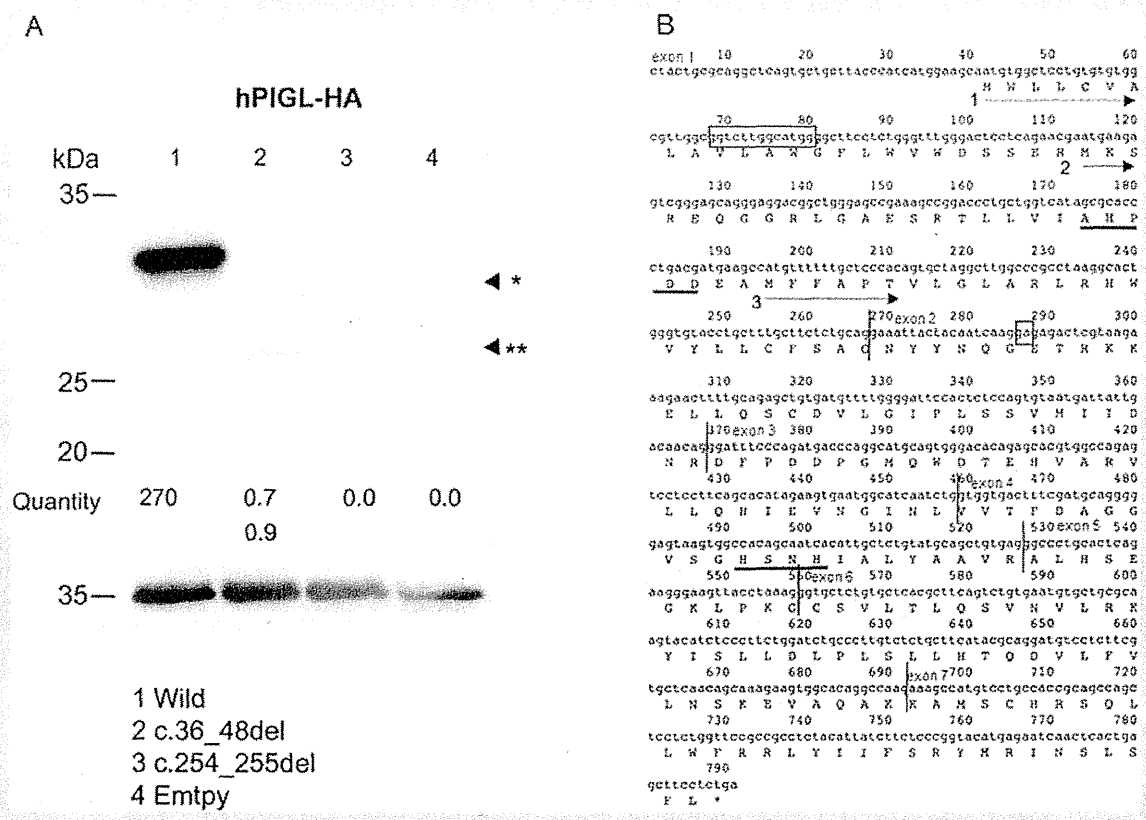

FIG. 5. Functional analysis. A: Lysates were separated by SDS–PAGE and western blotting was performed. Faint bands (* and **) could be detected from the lysate of the C-terminally tagged c.36_48 mutant transfected cells, which corresponded to the isoform starting from the down stream methionines (2 and 3 in Fig. 5B) that showed residual *PIGL* activity. No band could be detected from the lysate of the c.256_255 mutant tagged at either terminus. (Normalized with the intensities of GAPDH, the loading control, and luciferase activities used for evaluating transfection efficiencies). B: The sequence of *PIGL* cDNA; thick lines, conserved motifs; numbered arrows, three translation initiation sites; boxes, deletions in this patient.

deficiencies caused by a defect in the GPI-biosynthesis genes should show similar symptoms that result from the decreased expression of various GPI-APs on the cell surface. The severity depends on the amount of the GPI-anchor produced in ER, and the individual's genetic background may also have some influence on variations. Clinical manifestations in our patient were more similar to those in individuals with HPMRS, including hypertelorism, long palpebral fissures, broad nasal tip, tented upper lip, brachytelephalangy, severe intellectual disability and persistent hyperphosphatasia (Table I) [Horn et al., 2011]. These results suggest that frameshift mutations in 5′ terminus of *PIGL* cause HPMRS. It is possible that *PIGL* mutations identified in patients with CHIME syndrome might have higher residual activities.

Brain CT and MRI of our patient showed cerebellar atrophy. Frontotemporal atrophy and cerebellar hypoplasia have been shown in patients with *PIGT* mutations [Kvarnung et al., 2013]. Cerebral and cerebellar atrophy have been reported in a patient with *PIGO* mutation [Nakamura et al., 2014] and in patients with *PIGN* mutations [Maydan et al., 2011; Ohba et al., 2014], suggesting that cerebral atrophy and cerebellar atrophy are common features in patients with inherited GPI deficiencies. It is of note that cerebral atrophy has been also observed in patients with CHIME syndrome [Shashi et al., 1995; Schnur et al., 1997].

Our previous study demonstrated that mutant CHO cells having defects in the later step genes efficiently secrete ALP into the medium, whereas most ALP produced in the early step mutants is degraded in the cells [Murakami et al., 2012] because GPI transamidase is activated through binding with a mannose-containing GPI intermediate before this enzyme complex processes the precursor proteins for release. However, there are cases that are inconsistent with these experimental results. Some *PIGA*-deficient patients showed mild elevation of ALP (412 IU/L, normal range, 39–117 IU/L) [Johnston et al., 2012]. Elevation of ALP has not been reported in previously reported patients with *PIGL* deficiencies [Ng et al., 2012]. There may be differences in in vitro culture and in vivo body conditions; however, the primary reason for these differences needs to be identified in the future.

TABLE I. Summary of Clinical Features in Our Patient and HPMRS Patients With *PIGV*, *PIGO*, *PGAP2*, *PGAP3*, and *PIGW* Mutations

	Our study (PIGL)	PIGV	PIGO	PGAP2	PGAP3	PIGW
References		Horn et al. [2011]; Krawitz et al. [2010, 2012]	Krawitz et al. [2012]	Krawitz et al. [2013]; Hansen et al. [2013]	Howard et al. [2014]	Chiyonobu et al. [2014]
Sex	1 female	9 females and 5 males	3 females	4 female and 1 male	4 females and 2 males	1 proband
Age at assessment	1 year 10 months	7 months–17 years	20 months–15 years	3.5 and 28 years	2–17 years	ND
Origin	Japanese	German, Moroccan, Dutch, Polish, British, and European American	European	Finnish, Turkish, Northwestern Syria and Pakistani	Pakistani, American and Saudi–Arabian	Japanese
Height	−1.0 SD	normal in 13/14	−1.4 to −4.2 SD	−0.9 to 0.6 SD	normal in 4/5	ND
Weight	−2.0 SD	normal in 13/14	+0.6 to −3.3 SD	−1.0 SD to normal	normal in 4/5	ND
OFC	−1.0 SD	normal in 12/14	+0.7 to −5.5 SD	−4.5 SD to normal	−3.0 SD to normal	ND
Hyperphosphatasia	+	14/14	3/3	4/4	5/5	+
Intellectual disability	severe	14/14	3/3	4/4	5/5	+
Age at walking	delayed	delayed	delayed	5/5	delayed unable to walk in 4/5	ND
Delayed speech and language development	+	14/14	3/3	4/5	5/5 (none)	+
Muscular hypotonia	+	11/12	3/3	4/5	5/5	ND
Seizures	+	9/12	1/3	2/5	4/5	+
Apparent hypertelorism	+	+	3/3	1/2	5/5	ND
Long palpebral fissures	+	+	3/3	1/2		ND
Broad nasal tip	+	+	3/3	2/2	5/5	+
Tented upper lip vermilion	+	+	3/3	1/2	5/5	+
Brachytelephalangy	+	14/14	3/3	1/2	0/5	−
Anorectal abnormalities and/or constipation	−	6/12	3/3	1/2	ND	−
Aganglionic megacolon	−	2/14	1/3	1/2	ND	−
Heart defect	−	1/14	+	1/2	ND	−
Cleft palate	−	3/14	0/3	1/2	ND	−
Hearing impairment	+	3/14	0/3	1/2	ND	ND

ND, not described.